Mineralogy and Petrology (1998) 64: 119–147

Mineralogy and Petrology

Evolution of fluids responsible for iron skarn mineralisation: an example from the Vyhne-Klokoč deposit, Western Carpathians, Slovakia

P. Koděra[1,2], **A. H. Rankin**[2], and **J. Lexa**[1]

[1] Geological Survey of the Slovak Republic, Bratislava, Slovakia
[2] School of Geological Sciences, Kingston University, Kingston-upon-Thames, United Kingdom

With 14 Figures

Received April 9, 1998;
revised version accepted June 15, 1998

Summary

Vyhne-Klokoč, the largest Fe-skarn deposit in the Western Carpathians, is related to the emplacement of a large granodiorite pluton in the central zone of a Neogene stratovolcano. Skarn mineralisation is developed in places where apophyses of the pluton intruded basement carbonates. Granodiorite in the apophyses grades into rocks of granitic composition, involving the replacement of mafic minerals and a concomitant decrease in Fe-content. Ca-magnetite exoskarns (not accompanied by endoskarns) developed in three paragenetic stages. Fluid inclusion (FI) data for quartz in granodiorite suggest the existence of aqueous fluid immiscibility during the early hydrothermal stages. Three end-members of FIs were recognised, with a continuum between all three types. High salinity, liquid-rich, probably secondary FIs (29–68 wt % NaCl eq., Th 450 to 570 °C, composed of NaCl+$FeCl_2$+KCl) coexist with vapour-rich FIs with low but variable salt contents (±CO_2). Probably late secondary FIs (1–25 wt % NaCl eq., composed mainly of NaCl+$CaCl_2$, Th 188–283 °C) form the other end-member type of FIs trapped in granodiorite quartz. FIs from skarn garnets show a large variation in salinity (4–23 wt % NaCl eq., composed of NaCl±$FeCl_2$+$CaCl_2$+KCl+$MgCl_2$) and Th (220–370 °C), independent of the garnet types, probably reflecting variable amounts of magmatic fluids and low salinity meteoric waters. FIs in retrograde quartz, calcite and sphalerite show progressively more dilute (0–4 wt % NaCl eq, Th 215–380 °C), probably dominantly meteoric fluids with evidence for boiling at shallow depth. Chlorite crystallisation temperatures, calculated from the chlorite geothermometer, are in good agreement with the Th data for FIs in associated skarn minerals. Compositional changes in the granodiorite apophyses are the result of

subsolidus autometasomatic reactions of accumulated saline magmatic fluid inside the apophyses with pre-existing mafic mineral phases. Reactions add the iron to the fluid – the potential source for magnetite skarn. Later mixing with dilute, cooler probably meteoric waters had the effect of decreasing the salinity and density of the equilibrated magmatic fluid, making it more buoyant and capable of moving out from the apophyses into the country rocks, causing metasomatic reactions and precipitating magnetite. An overlap exists between the FI microthermometry data from *primary* FIs in garnets and late *secondary* FIs in the granodiorite quartz indicating the same sources of the hydrothermal fluids – probably mixtures of magmatic and meteoric waters. Based on fluid inclusion, geological, petrological and mineralogical data, an integrated fluid evolution model involving magmatic and meteoric fluids is developed to explain the geological and fluid controls on Fe-skarn mineralization associated with granodiorite intrusions.

Zusammenfassung

Die Evolution von Fluiden bei Fe-Skarn Mineralisation: Ein Beispiel von der Lagerstätte Vyhne-Klokoč, West-Karpathen, Slowakei.

Vyhne-Klokoč ist die größte Fe-Skarn Lagerstätte in den Westkarpathen. Sie steht in Beziehung zur Platznahme eines großen Granodiorit-Plutons in der Zentralzone eines neogenen Stratovulkans. Skarn-Vererzung ist dort zu finden, wo Apophysen des Plutons Karbonate des Basements intrudieren. In den Apophysen geht Granodiorit in Gesteine granitischer Zusammensetzung über, wobei mafische Minerale verdrängt werden und der Fe-Gehalt abnimmt. Ca-Magnetit-Exoskarne (nicht von Endoskarnen begleitet) entstanden in drei paragenetischen Stadien. Flüssigkeits-Einschluß-Daten (FI) für Quarz in Granodiorit weisen auf Unmischbarkeit von Fluiden während der frühen hydrothermalen Stadien hin. Drei Endglieder von FI liegen vor, die durch Kontinuum miteinander verbunden sind. Hochsalinare, wahrscheinlich sekundäre FI mit hohem Anteil fluider Phase (29–68 wt % NaCl eq., T_h 450–570 °C; bestehend aus NaCl+$FeCl_2$+KCl) koexistieren mit Gas-reichen FI mit niedrigem aber variablem Salzgehalt (±CO_2). Sekundäre, wahrscheinlich spät gebildete FI (1–25 wt% NaCl eq., Hauptbestandteile NaCl+$CaCl_2$, T_h 188–283 °C) bilden das andere Endglied von FI in Granodiorit-Quarz.

FI aus Skarn-Granaten zeigen größere Variationen der Salinität (4–23 wt % NaCl eq., Hauptkomponenten NaCl±$FeCl_2$+$CaCl_2$+KCl+$MgCl_2$) und T_h (220–370 °C). Diese Zusammensetzungen sind unabhängig von der Art der Granate und dürften das Ergebnis von Mischung variabler Mengen magmatischer Fluide und meteorischer Wässer niedriger Salinität sein. FI in retrogradem Quarz, Calcit und Sphalerit zeigen zunehmend mehr verdünnte (0–4 wt% NaCl eq., T_h 215–380 °C), wahrscheinlich großteils meteorische Fluide mit Hinweisen auf Kochen in geringer Tiefe. Temperaturen für die Kristallisation von Chlorit wurden mit dem Chlorit-Geothermometer ermittelt; diese stimmen gut mit T_h-Werten für FI in assoziierten Skarn-Mineralen überein. Änderungen der Zusammensetzung der Granit-Apophysen sind das Ergebnis von autometasomatischen Subsolidus-Reaktionen magmatischer Fluide, die sich in den Apophysen angesammelt haben, mit präexistierenden mafischen Mineralen. Solche Reaktionen erhöhen den Fe-Gehalt in den Fluiden – die potentielle Quelle für Magnetit-Skarne. Spätere Mischung mit verdünnten, kühleren Fluiden, wahrscheinlich meteorischer Herkunft, senkte Salinität und Dichte der magmatischen Fluide und erleichterte so ihren Aufstieg in die Nebengesteine. Dies führte zu metasomatischen Reaktionen und zur Ausfällung von Magnetit. Mikrothermometrische Daten von

primären FI in Granat und von sekundären FI in Granodiorit-Quarz überlappen teilweise und weisen auf ähnliche Ausgangs-Fluide hin, wahrscheinlich Mischungen magmatischer und meteorischer Wässer. Geologische, petrologische, mineralogische und FI-Daten ermöglichen die Entwicklung eines integrierten Modells für die Fluid-Evolution bei der Bildung von Fe-Skarnen in Granodiorit-Intrusionen.

Introduction

Skarn deposits are an important type of mineralisation closely associated with acid to intermediate magmatism. They typically occur at or near the contact between igneous intrusions and carbonate rocks. Classical theories for the genesis of skarns and associated mineralisation envisage a multistage evolution connected to late magmatic and associated hydrothermal activity (e.g. *Einaudi* et al., 1981; *Einaudi* and *Burt*, 1982; *Pirajno*, 1992).

Fluid inclusion studies provide an effective method of investigating PVTX properties and the evolution of fluids involved in skarn formation. Previous studies have shown that these fluids are typically of variable salinity but frequently show a characteristic dilution or mixing trend from high temperature, high salinity (magmatic ?) fluids to lower temperature, dilute (meteoric) fluids (*Roedder*, 1984; *Kwak*, 1986; *Layne* and *Spooner*, 1991; *Jamtveit* and *Andersen*, 1993). The published fluid inclusion data are in agreement with recent experimental and theoretical models for fluid evolution in magmatic systems (e.g. *Burnham*, 1979; *Whitney* et al., 1985; *Shinohara* et al., 1989; *Candela*, 1991). Although a general model is now accepted for skarn mineralisation, the relationship between the evolution of magmatic fluids inside the pluton and the skarn-forming and mineralising processes in the evolving skarn environment is still not yet clear.

As a part of a wider project on "Mineral resources of Slovakia" (*Onačila* et al., 1995), investigating the metallogenetic evolution of the Banská Stiavnica ore district within the Central Slovakia Neogene Volcanic field, a detailed mineralogical, petrological and fluid inclusions study of the Vyhne-Klokoč iron skarn deposit has been carried out. The geological setting, mineralogy and geochemistry of the deposit are particularly well established (*Gavora*, 1962; *Gavora* and *Hruškovič*, 1963; *Gavora* and *Lukaj*, 1968; *Konečný* et al., 1993; *Káčer* et al., 1993; *Koděra* and *Chovan*, 1994; *Koděra*, 1994) and the deposit provides an excellent opportunity of investigating the link between fluids associated with skarn mineralization and associated granodiorite. Here we report new data on fluid inclusions in paragenetically well-constrained stages of skarn mineralisation, together with data on the inclusion populations in the associated granodiorite. From the combined fluid inclusion and paragenetic results, and a summary of available geological and petrological data a new fluid evolution model is developed for skarn development in this type of setting.

Geological setting

The Vyhne-Klokoč magnetite deposit is part of the Hodruša-Štiavnica ore district. This district, with historical production of gold, silver, base metals and iron,

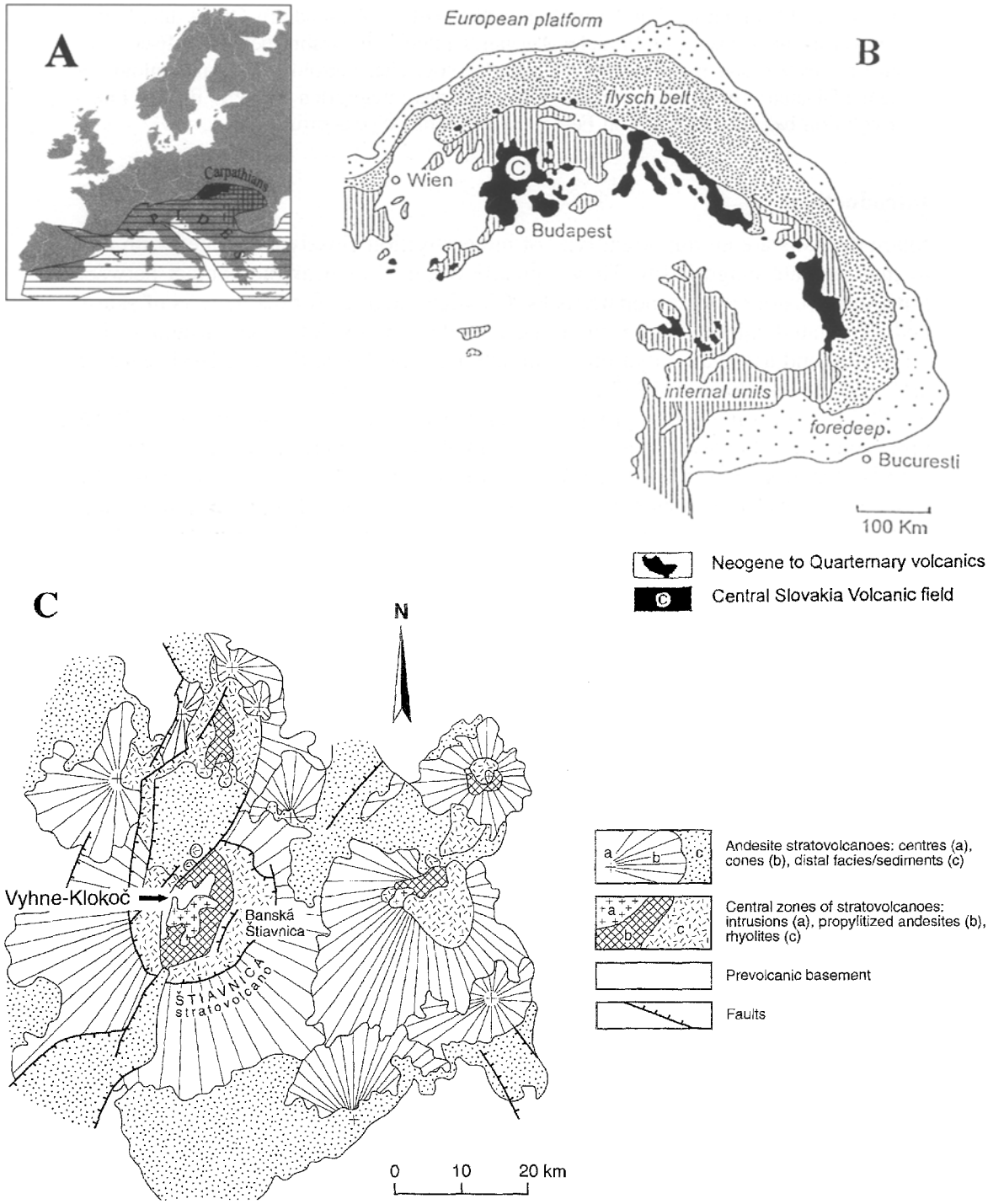

Fig. 1. **A** Regional setting of the Carpathian Arc inside the Alpides of Europe (cross-hatched) and Slovakia (black) **B** Position of the Central Slovakian Neogene Volcanic Field in the Carpatho-Pannonian region **C** Structure of the Central Slovakian Neogene Volcanic Field with location of the Banská Štiavnica stratovolcano and the Vyhne-Klokoč skarn deposit

contains a variety of mineralisation types ranging from intrusion related, subvolcanic skarns and porphyry copper systems to high level epithermal base and precious metal veins.

The Hodruša-Štiavnica ore district is hosted in the central zone of a large andesite stratovolcano (Štiavnica stratovolcano) – the most extensive one in the Central Slovakia Neogene Volcanic Field (Fig. 1). Volcanic activity, which is of high-K calc-alkali type, comparable with andesite volcanoes of continental margins (*Lexa* et al., 1993), was related to subduction and back-arc extension processes within the Carpathian arc. The structure, stratigraphy and evolution of the Štiavnica stratovolcano is described by *Konečný* et al. (1983, 1995) and the geology of the Hodruša-Štiavnica ore district by *Lexa* et al. (in press). The stratovolcano comprises mainly pyroxene and hornblende-pyroxene andesites. The central zone is represented by a caldera 20 km in diameter, filled by a biotite-hornblende andesite dome/flow complex. Evolution of the volcano took place between 16.3–10.5 Ma (*Konečný* et al., 1983; *Lexa* et al., in press). A resurgent horst in the centre of the caldera brings to the surface basement rocks and an extensive subvolcanic intrusive complex. This complex is dominated by a granodiorite pluton, emplaced during the precaldera stage of volcano evolution (16.3–15.5 Ma, *Lexa* et al., in press). Owing to the alteration and thermal overprint by a younger epithermal system, attempts to date the granodiorite by radiometric methods have not been successful (*Rozložník* et al., 1991). The complex is emplaced into a basement of Hercynian granite and schists, overlain by a cover sequence of Middle to Upper Triassic carbonate sediments (Vel'ký Bok Group) overthrust by late Paleozoic to Late Triassic clastic and carbonate sediments of the Choč nappe.

Generally, Fe-skarn mineralisation occurrences are spatially limited to those areas where basement rocks with carbonate sequences at the roof of the Neogene granodiorite pluton were brecciated and intruded by apophyses of the intrusion (*Lexa* et al., in press).

The Vyhne-Klokoč deposit is the largest Fe-skarn locality in this district, as well as in whole of the Western Carpathians, with 2.6 million tons of proven magnetite reserves (*Gavora* and *Lukaj*, 1968). The deposit is situated in the NW part of the central zone of the stratovolcano, about 2.5 km SW from the village of Vyhne (Fig. 1c). The schematic map and cross-section shown in Fig. 2a and b (*Káčer* et al., 1993) are based on exploration drill holes, underground development (*Gavora* and *Lukaj*, 1968) and recent geological surveys (*Konečný* et al., 1993). The cross-section shows the close relationship between skarn development, limestones and the granodiorite intrusion, including its apophyses. The apophyses intrude both the skarnised limestones of the Vel'ký Bok Group and overlying rocks of the Choč nappe (Fig. 2a). The main skarn bodies occur in limestones as irregular lenses up to about 35 metres thick and 500 metres long. They dip at up to 60° to the West, subparallel to the dip of the granodiorite contact (*Gavora* and *Hruškovič*, 1963). Skarns are cut by younger (post-mineralisation) quartz diorite porphyry dykes with chilled contacts against rocks that include skarns. Remnants of an Hercynian granite in places separates the skarn-hosting carbonates from the main body of granodiorite. However, at other skarn occurrences in the Štiavnica-Hodruša district, there is a direct contact of granodiorite and skarns with both endo- and exoskarns being present.

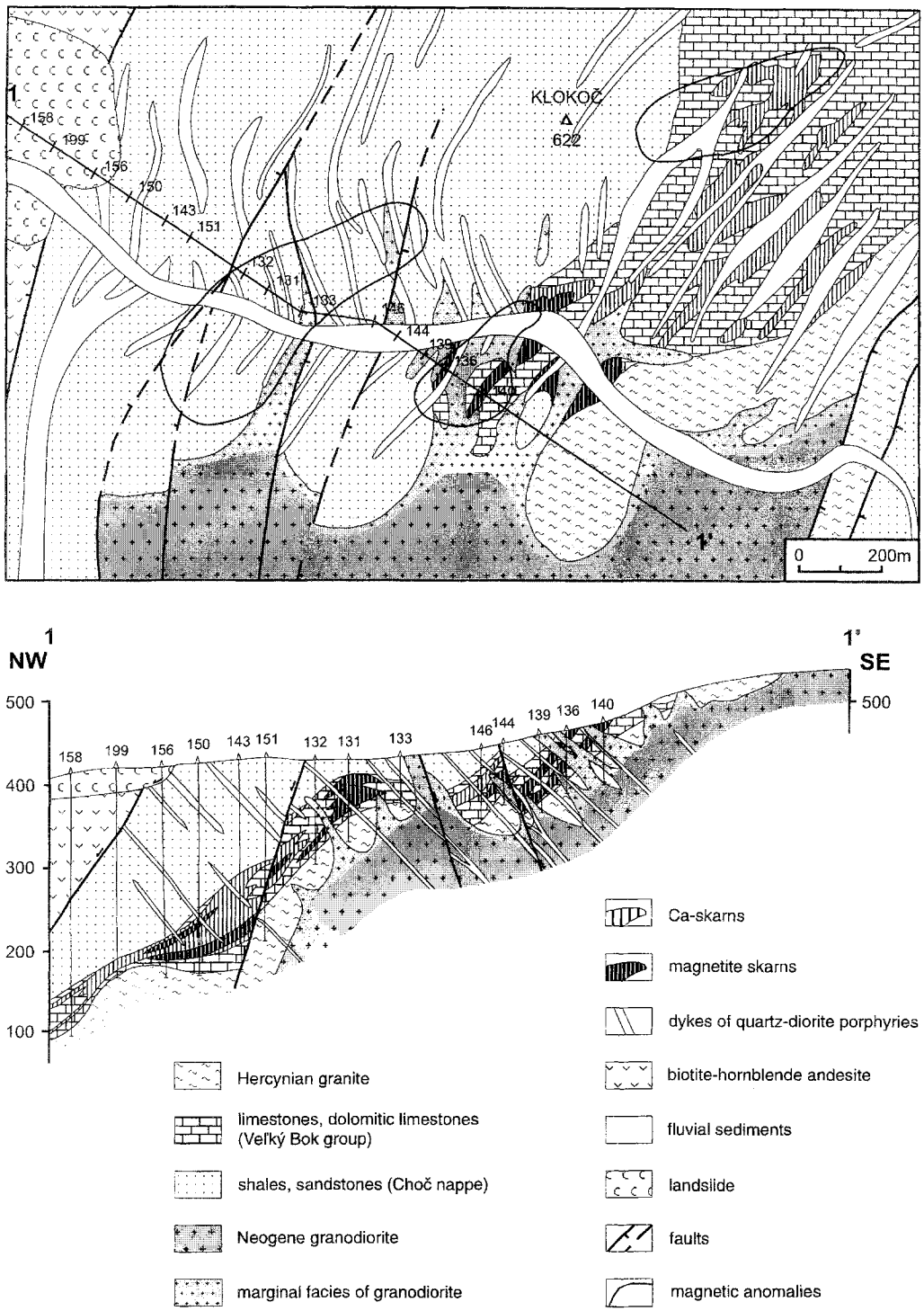

Fig. 2. Geological map and cross section of the Vyhne-Klokoč iron skarn deposit, based on geological survey, exploration drill holes and underground development. Magnetic anomalies shown in the geological map indicate magnetite ores in the underground

Petrology and alteration patterns

The host sedimentary carbonates of the Vel'ký Bok group are typically fine grained, Fe-poor, calcic and dolomitic limestones. Close to the contact with the granodiorite these limestones are recrystallised to marble and strongly affected by the skarnification process with the development of characteristic skarn minerals (including magnetite) as discussed below. The skarns show distinctive mineral zoning away from the granodiorite contact with magnetite-bearing skarns occurring closest to the contact (*Gavora* and *Hruškovič*, 1963).

Throughout the ore district the apophyses of the granodiorite pluton change composition towards the basement/granodiorite contact (Fig. 2b, Table 1). The fresh granodiorite typically has a crystal size of 3 to 6 mm and consists of idiomorphic (sometimes partially resorbed) amphibole and biotite, hypidiomorphic plagioclase (An_{60-30}), and allotriomorphic to poikilitic K-feldspar and quartz. Textural and modal composition of the granodiorite indicates that, at the time of emplacement, the magma was composed of approximately 40 to 50% plagioclase, amphibole and biotite phenocrysts in a silicate liquid close to the eutectic composition (*Šulgan*, 1986).

In the apophyses (at the basement/granodiorite contact) there is a local increase in size and abundance of the K-feldspar and quartz owing to replacement of plagioclase and mafic minerals. Plagioclase is partially replaced also by an albite-rich variety (An_{30}) and mafic minerals are chloritised. The $KAlSi_3O_8$ content of K-feldspar increases to 95%, indicating subsolidus exchange with K-rich fluids. Granophyric intergrowths of K-feldspar and quartz have been observed near the contact as a result of the undercooling of the melt caused by escape of aqueous phases (*Káčer* et al., 1995). The metasomatic replacement of mafic minerals is reflected in a distinct decrease in the Fe-content in the granodiorite apophyses towards the contact zone (Table 2, Fig. 3), indicating the likely source of iron in

Table 1. *Mineralogy and alteration patterns of different types of granodiorite. Mineral mode of the pluton changes towards the contact with country rocks involving total replacement of mafic minerals in apophyses as the result of autometasomatic subsolidus reaction*

Granodiorite type	Mineralogy & alteration
Apophyses	– more K-feldspar, quartz, albite rich plagioclase – total replacement of mafic minerals – granophyric intergrowths of K-feldspar and quartz – feldspars replaced by sericite, clays (hydrothermal event)
Transitional	– local increase in size and abundance of K-feldspars – albititisation of plagioclase – chloritisation of mafic minerals
Fresh	– idiomorphic amphibole, biotite – hypidiomorphic plagioclase – allotriomorphic K-feldspar, quartz

Table 2. *Typical whole rock chemical analyses of fresh granodiorite (1), its altered apophyse (2) and aplite differentiate (3) from the Central zone of the Banská Štiavnica stratovolcano. Data from* Lexa *et al. (1997)*

	1	2	3
SiO_2	61.35	63.85	76.84
TiO_2	0.62	0.62	0.16
Al_2O_3	16.56	16.74	12.32
Fe_2O_3	1.78	0.91	0.43
FeO	3.81	1.85	0.65
MnO	0.11	0.05	0.01
MgO	2.34	1.92	0.04
CaO	5.23	5.55	0.62
Na_2O	3.10	3.81	2.18
K_2O	3.29	3.45	6.09
P_2O_5	0.27	0.12	0.02
S total	0.01	0.13	0.01
H_2O +	1.34	0.68	0.39
H_2O -	0.13	0.19	0.15
Total	99.93	99.87	99.91
Rb	58	66	106
Sr	430	540	124
Ba	698	635	96
Zr	137	123	75
Y	19	14	2
Nb	13	2	18
Ta	0.8	0.4	0.6
Ni	8	13	12
Co	12.0	7.1	5.7
Cr	27.0	14.0	31.0
V	120	80	10
Cu	5	26	8
Pb	2	8	19
Zn	62	39	80
Hf	3.4	2.0	4.0
Th	8.4	5.7	9.1
U	0.2	<0.4	<0.6
La	30.2	14.5	21.2
Ce	50.2	31.1	52.3
Nd	1	11	19
Sm	4.68	2.79	3.80
Eu	0.93	0.61	0.99
Tb	0.5	0.3	0.5
Yb	2.10	1.20	2.00
Lu	0.25	0.19	0.33

magnetite skarns (as discussed later). The behaviour of other major elements is not as clear, but generally Ca and Na increase toward the contact, while Si, Al and K remain unchanged (Table 2). In the contact zone feldspars also show alteration to sericite and clay minerals, but this appears to represent a superimposed hydrothermal event (reported in *Káčer* et al., 1995).

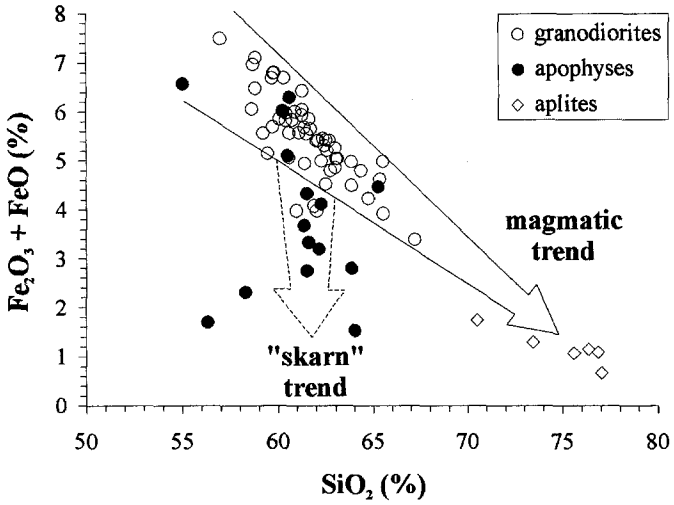

Fig. 3. SiO_2 vs. Fe_{total} diagram for granodiorites, granodiorite apophyses and aplites from the Central zone of the Banská Štiavnica stratovolcano. Sample analyses are shown in Table 2. A distinct decrease in the rock Fe-content of the granodiorite apophyses is reflected in the "skarn" trend, indicating the likely source of iron in magnetite skarns. Data from *Lexa* et al. (1997)

The Hercynian basement granite is affected by recrystallization, as well as by local fracturing and brecciation. These fractures are filled by a tourmaline-quartz assemblage and are probably the result of a granodiorite contact effect (*Káčer* et al., 1993).

Mineralogy of the skarn

Within the whole Hodruša-Štiavnica ore district many types of skarns are recognised. Mg-skarns and Ca-skarns are both developed on exo-and endocontacts (*Zábranský*, 1969; *Káčer* et al., 1993). The Vyhne-Klokoč deposit is classified as a pure *Ca-magnetite exoskarn*, with no evidence for either Mg-skarn or endoskarn mineralisation (*Koděra*, 1994; *Koděra* and *Chovan*, 1994).

Previous studies (*Koděra*, 1994; *Koděra* and *Chovan*, 1994) have proposed a sub-division of the main skarn-forming stage according to the classic scheme of *Einaudi* et al. (1981) starting with an initial isochemical stage followed by metasomatic and retrograde stages. Several paragenetic stages of later hydrothermal mineralization were also recognised. A simplified version of the paragenetic chart of *Koděra* and *Chovan* (1994) is presented in Fig. 4. Stages have been omitted partly for clarity but also because no clear spatial zonal arrangements of skarn mineral assemblages could be recognised in many samples suitable for fluid inclusion studies (often only mine dump material was available to study).

The earliest stages of skarn formation involved the crystallisation of non-hydrous silicates, especially zoned garnets (grossularite-andradite series), rare pyroxenes (diopside-hedenbergite series), wollastonite and clinochlore, in the marginal zones. During the main phase of skarn formation Fe-enriched minerals,

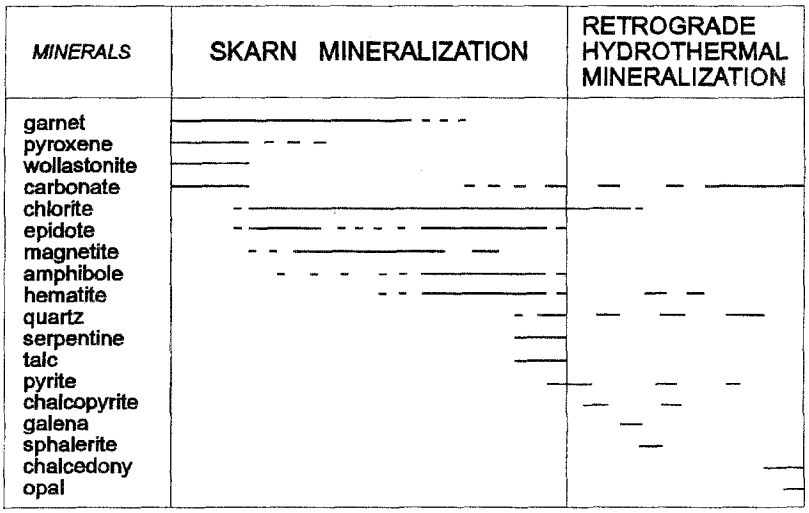

Fig. 4. Paragenetic chart for mineral growth in the Vyhne-Klokoč skarn deposit (simplified from *Koděra* and *Chovan*, 1994)

especially magnetite, garnet (dominantly andradite), epidote, tremolite and Fe-clinochlore, were developed. Magnetite replaces marbles and earlier skarn mineral assemblages (including garnet, tremolite, epidote and clinochlore). The last phase of skarn development saw the crystallisation of strongly zoned garnet, major hematite and minor magnetite, epidote, amphibole (dominantly actinolite), various chlorites and other minerals. Subsequent *retrograde hydrothermal mineralisation* involved a pronounced development of pyrite-chalcopyrite followed by base metal mineralization. This is spatially related to, but not contemporaneous with the skarn, that involves the strong development of garnet. The later stages (calcite-hematite, quartz-carbonate, chalcedony-opal) occur mostly as fracture fillings.

The following brief description of skarn minerals, based mainly on *Koděra* (1994) and *Koděra* and *Chovan* (1994), focusses only on those minerals, important for interpretation of the fluid inclusion (Fl) data. Three types of garnet, all belonging to the grossular-andradite series (Ad_{22-100}, Sp_{0-4}), have been distinguished both texturally and chemically (Fig. 5). Early garnet (garnet I) is extensively zoned, anisotropic, often altered and replaced by magnetite. Garnet II is dominantly andraditic ($=Fe^{+3}$ rich), isotropic, with rare "more grossularic" zones. Locally it is replaced by magnetite, with which it usually appears coeval. Garnet III is also extensively zoned and often occurs as veinlets cutting earlier skarn assemblages (including earlier garnet generations). Most of the zones are anisotropic with increased Mn content in the outermost zones.

Chlorites show a wide range of mineral compositions representing different generations. According to the nomenclature of trioctahedral chlorites (*Bayliss*, 1975) all belong to the group of clinochlore with various content of Fe^{+2}, Mg and Si. Chlorite A is the earliest, fine grained, nearly pure clinochlore, often replaced by magnetite. Chlorite B is fine grained Fe-clinochlore associated with late garnets and retrograde skarn assemblages. It is occasionally replaced by magnetite. Chlorite C is the latest coarse grained variety of clinochlore (Mg, Si-clinochlore). It

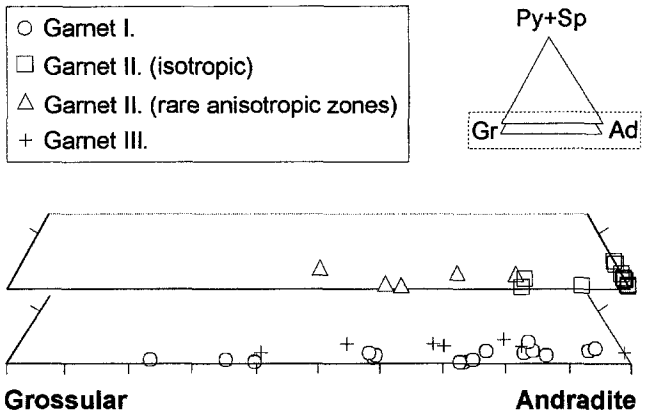

Fig. 5. Ternary diagram of garnet composition, based on microprobe analyses (*Koděra* and *Chovan*, 1994). *Gr* grossular, *Ad* andradite, *Py* pyrope, *Sp* spessartine

occurs in veinlets and vugs in coarse grained magnetite. As the composition of chlorite is very sensitive not only to the fluid composition but also to the temperature, the chlorite geothermometer proposed by *Cathelineau* and *Nieva* (1985) and corrected by *Cathelineau* (1988) can be used to broadly compare the data from the fluid inclusion microthermometry in skarn minerals (see below). Figure 6 shows the relationship between the approximate crystallisation temperature of different generations of chlorites (calculated from microprobe analyses of *Koděra* and *Chovan*, 1994) and their Fe^{+2} content. The Fe^{+2} and Fe^{+3} proportions were determined from the charge balance, assuming 10 O and 8 (OH+F+Cl) using the microcomputer program MINFILE (*Afifi* and *Essene*, 1988). These calculations

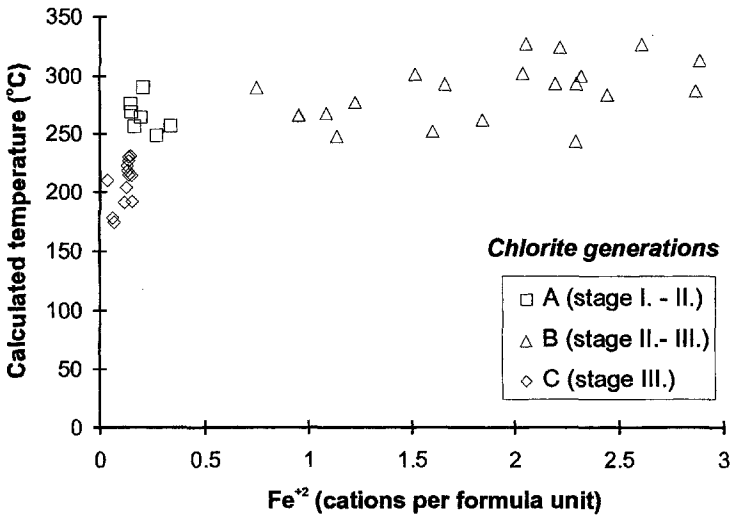

Fig. 6. Temperature vs. Fe^{+2} diagram for different generations of chlorites at the Vyhne-Klokoč deposit based on microprobe analyses (*Koděra* and *Chovan*, 1994). Crystallisation temperature (T) of chlorites was calculated using the geothermometer proposed by *Cathelineau* (1988) based on the relationship between T and Al_{IV}: $T\ (°C) = -61.92 + 321.98\ (Al_{IV})$

showed that all the iron in chlorites can be regarded as Fe^{+2}. The geothermometer suggests reasonable crystallisation temperatures for all three generations, representing different stages of skarn evolution. The values (249–291 °C for A-chlorites and 244–328 °C for B-chlorites) are in good agreement with data reported here for fluid inclusions in skarn minerals. The large variation of Fe^{+2} in B-chlorites is possibly related to the large variation in salinity of the metasomatic and retrograde fluids (see fluid inclusion data below), as the iron solubility in aqueous fluids depends mainly on the salinity and less on the temperature (*Whitney* et al., 1985; *Kwak* et al., 1986). Crystallisation temperature of C-chlorites (175–231 °C) indicates late hydrothermal retrograde conditions, as already suggested by the paragenetic studies. It is likely, that low Fe contents of the C-chlorites is the result of earlier crystallisation of magnetite.

Epidote is common in the deposit. Early epidote is usually fine grained and replaced by magnetite. Retrograde epidote is coarse grained and is often present in thin veinlets cutting earlier skarn assemblages.

Quartz and carbonates (mostly calcite and dolomite) are also common. Texturally, they appear to have crystallised only during the retrograde and retrograde hydrothermal stages of skarn evolution.

Sphalerite is relatively rare. Small crystals occur most often in the retrograde hydrothermal assemblage (base metal substage).

Fluid inclusions petrography and microthermometry

Methods

Fluid inclusion (FI) studies were carried out on a range of skarn minerals including garnet, epidote, sphalerite, quartz, calcite as well as from quartz from the least altered samples of the granodiorite, directly beneath the zone of skarn mineralisation. Prior to microthermometric analysis, a thorough optical and petrographic examination of the FI population was carried out. Where possible the inclusions were assigned a probable primary or secondary origin according to the criteria of *Roedder* (1984).

Temperatures of phase transitions were measured on selected inclusions with a Linkam heating-freezing stage THMSG-600 at Kingston University and at the Geological Survey of the Slovak Republic. The precision and accuracy of the microthermometric measurements (including inter-laboratory differences), based on standard calibration procedures, is estimated at ±0.3 °C for temperatures below −50 °C and at ±3 °C for temperatures near 350 °C. Homogenisation temperatures (Th), eutectic or first melting temperatures (Te), last ice melting temperatures (Tm_{ice}) and dissolution temperatures of daughter minerals (Tm_x) were measured where possible on the aqueous inclusions. In a few vapour-rich FIs the temperature of partial homogenisation of a CO_2-rich phase ($ThCO_2$) and its melting temperature ($TmCO_2$) were measured. Attempts to record clathrate melting temperatures in these inclusions were unsuccessful. Salinities (expressed as wt.% NaCl eq.) were estimated from the last ice melting temperatures using the microcomputer program PVTX (equations of *Hall* et al., 1988) and from the halite daughter minerals melting temperatures using the program FLINCOR (*Brown*,

1989). Te values were used to constrain the likely gross composition of the solutions by comparison with published eutectics for various salt-water systems (*Shepherd* et al., 1985).

In situ qualitative analyses of individual solid phases from Fl were carried out using scanning electron microscope with an energy dispersive X-ray spectrometer (EDAX) at the Geological Survey of the Slovak Republic. Optical identification of one daughter mineral (ferropyrosmalite) was confirmed by Laser Raman analysis, carried out by Dr. *S. Roberts* of Southampton University.

The granodiorite

Preliminary microthermometric studies were carried out on 75 Fls in quartz from the least altered samples of the granodiorite near to the skarn contact. The Fls were abundant, generally less than 20 μm in size (15 μm in average), and showed a wide range of vapour/liquid/solid ratios (Fig. 7).

Based on SEM-EDS, optical and microthermometric observations, the following solid phases have been identified: halite, sylvite, Fe-chloride, K-Fe chloride, Fe-K chloride, magnetite, hematite (Fig. 7a, b, e). Halite is dominant and ubiquitous in nearly all Fl with true daughter minerals (DM). Magnetite was identified by its magnetic properties and hematite by its typical red colour. Both minerals are interpreted as captive minerals (CM), because they occur only occasionally with variable phase ratios in all types of Fls and they always failed to dissolve on heating (*Shepherd* et al., 1985).

The mineralogy of various mixed K-Fe-Cl phases is complex and difficult to characterise completely. The most common iron-bearing DMs are typically pale yellow to green, anisotropic with high relief and dissolve readily on heating (62–94 °C) (Fig. 8). In comparison with the observations of *Wilson* et al. (1980) and *Quan* et al. (1987) most of these are probably $KFeCl_3 \cdot nH_2O$ and/or $K_2FeCl_5 \cdot H_2O$ – erythrosiderite. However, the simple Fe-chlorides, identified by SEM-EDS, display similar optical properties and heating behaviour (*Shepherd* et al., 1985; *Kwak* et al., 1986) making it very difficult to distinguish them from the more complex Fe-K-chlorides based on microthermometric observations alone. This is evident from experimental studies in the $FeCl_2$-H_2O system (*Schimmel*, 1928) showing that $FeCl_2 \cdot 4H_2O$ is the most likely stable phase at room temperature with a phase transition to the dihydrate at 75.6 °C. The other common iron-rich DM is usually prismatic green to yellow, anisotropic, with high relief. It dissolves usually between 450–572 °C (Fig. 8). Dissolution is sometimes accompanied by development of a new, unidentified, fibrous phase. This behaviour on heating is typical for ferropyrosmalite $(Fe,Mn)_8(OH,Cl)_{10}Si_6O_{15}$, which was confirmed by Laser Raman analysis (spectra compared to *Dong* and *Pollard*, 1997). Some of the other DMs dissolved in the interval 117–390 °C (Fig. 8) and according to SEM-EDS results and their optical properties are identified as sylvite or various K-Fe chlorides.

Based on optical, SEM and preliminary microthermometric studies three end-member types of Fls were recognised (Table 3, Fig. 9). These end-member types do not represent distinct groups or populations. A continuum probably exists among all three types, suggesting substantial evolution from immiscible, high salinity,

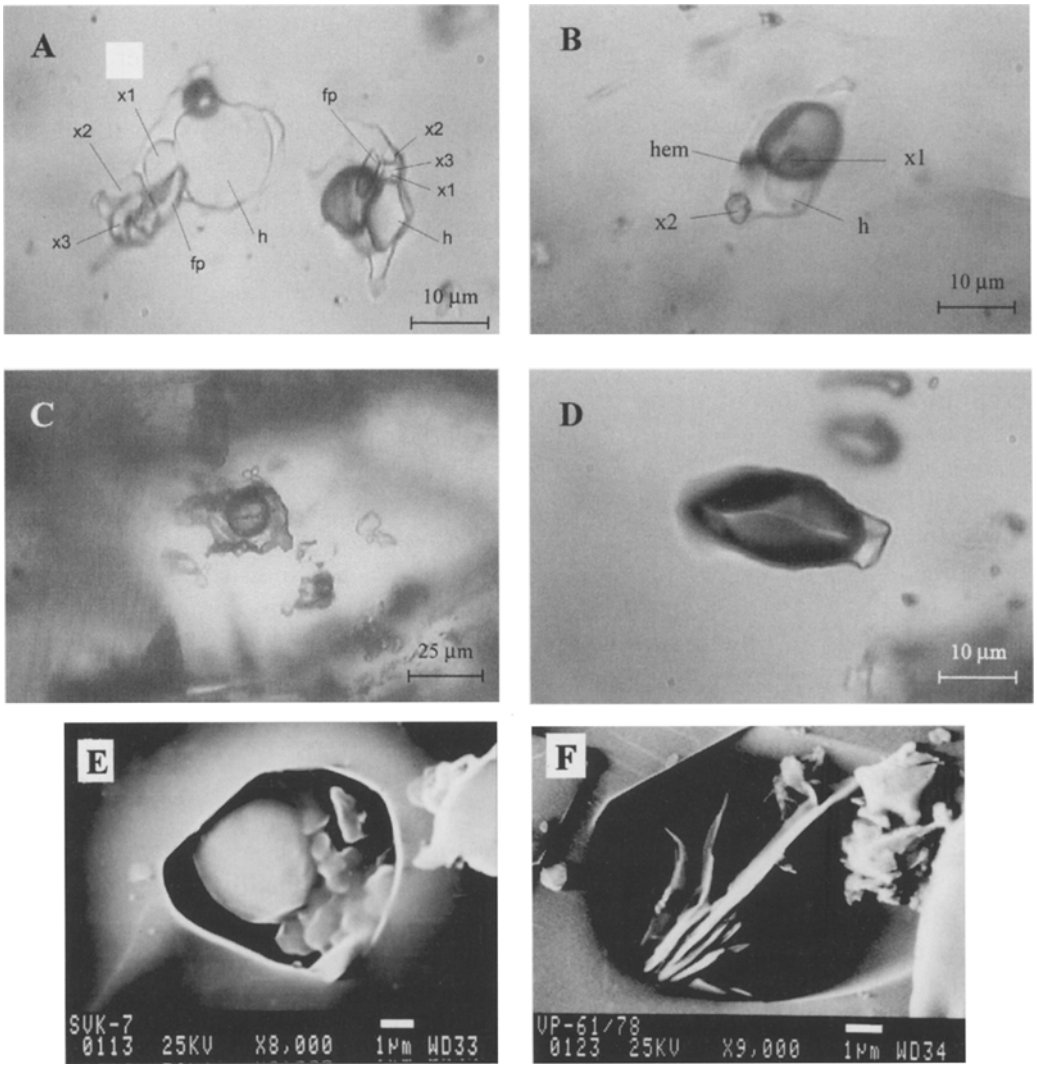

Fig. 7. Microphotographs of typical fluid inclusions (Fl) from the Vyhne-Klokoč skarn deposit: **A** Type I. liquid-rich multisolid Fl in granodiorite quartz with different degree of fill; **B** Type II. vapour-rich multisolid Fl in granodiorite quartz; **C** Primary liquid-rich Fl in early garnet I. (skarn); **D** Primary vapour-rich Fl in quartz from the boiling system (skarn); **E** SEM image of typical solid phases in open Fls in the granodiorite quartz; according to EDAX analyses the big round to cubic phase is halite, small hexagonal to round phases are K, Fe chlorides with different K : Fe ratio; **F** SEM image of captive fibrous minerals present in open Fl in quartz from skarn (sericite?). *h* halite, *fp* ferropyrosmalite (?), *hem* hematite, *x1–x3* various dissolving K, Fe chlorides

high temperature fluids to low salinity and cooler fluids (see discussion for more details).

Type I. (DM+L+V±CM) inclusions are liquid-rich (F = 0.7–0.9) and characterised by the presence of daughter minerals and occasional captive minerals (Fig. 7a). Solid phases sometimes occupy up to about 60% of the total volume of

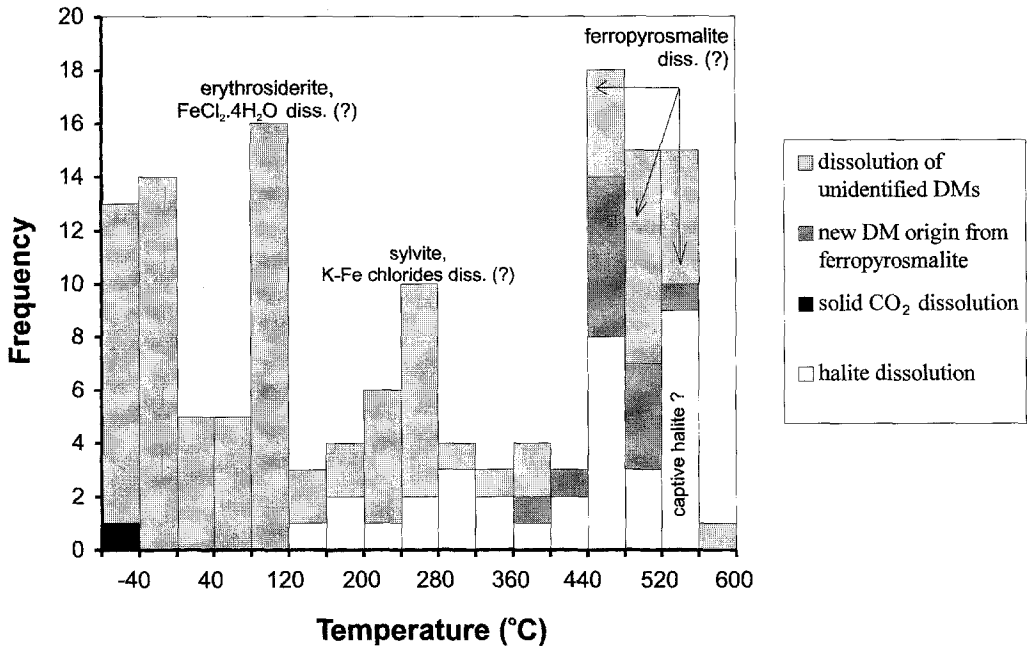

Fig. 8. Dissolution temperatures of daughter minerals (DM) in type I and II inclusions. Values below room temperatures represent dissolution of mostly unidentified salt hydrates, evolved during freezing. Dissolving DMs are probably erythrosiderite or $FeCl_2 \cdot 4H_2O$ (in the interval 60–120 °C); sylvite and/or various K-Fe chlorides (120–400 °C); ferropyrosmalite (450–560 °C). Dissolution of ferropyrosmalite is often accompanied by formation of a new unidentified stable phase. Some solid phases in Fls did not dissolve until ~600 °C

Table 3. *Summary of main microthermometric data from fluid inclusions in quartz from the granodiorite.* Tm-halite *temperature of halite dissolution*, Th-total *final homogenisation temperature*, Te *eutectic temperature*, n *number of inclusions measured*, L *liquid*, V *vapour*, DM *daughter mineral*, CM *captive mineral*

Fluid inclusion type	Tm - halite (°C)			Salinity (wt. % NaCl eq.)			Th - total (°C)			Te (°C)		
	n	range	mean	n	range	mean	n	range	mean	n	range	mean
I. (DM+L+V±CM)	27	144 ↔ 559	417	27	29.4 ↔ 68.0	51.3	30	204 ↔ 572	438	5	-53 ↔ -70	-59.4
II. (V+L±DM±CM)	7	186 ↔ 532	415	8	23.1 ↔ 64.2	48.0	2	390 ↔ 402	396	3	-52 ↔ -72	-62.3
III. (L+V±CM)	-	-	-	23	0.8 ↔ 24.6	10.5	22	188 ↔ 283	252	19	-28 ↔ -84	-55.1

the inclusions. The salinity varies from 29 up to 68 wt% NaCl eq., based on Tm_{halite}. Because of the likelihood of additional cations in the fluid, the Tm_{halite} is likely to be an underestimate of the bulk salinity. The total or final homogenisation (by vapour disappearance, by halite dissolution or by other DM dissolution) occurred from 204 to 572 °C. A few of the Fls with many DMs decrepitated before total homogenisation. Only some of the Fls froze totally during cooling; their low Te values (−70 to −53 °C) indicate the presence of $CaCl_2$ in the fluids.

Type II. (V+L±DM±CM) inclusions are vapour-rich (F = 0.7–0.2), with occasional daughter and/or insoluble captive minerals (Fig. 7b). In most cases, a

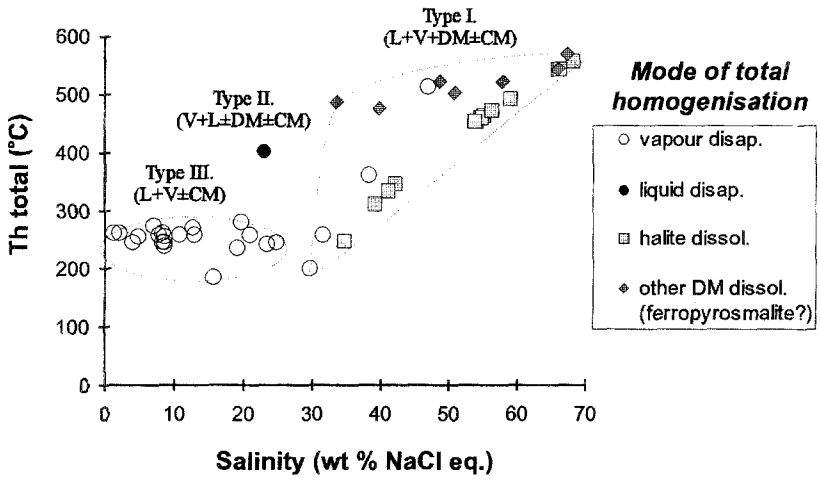

Fig. 9. Total homogenisation temperature (Th_{total}) vs. salinity diagram for fluid inclusions (Fl) in granodiorite quartz. Different types of Fls are plotted with various modes of final homogenisation. Note the continuum existing among all three types of Fls. Nearly all type II. inclusions (V+L±DM±CM) are missing because: i) most of the Fls did not show V/L homogenisation when heated up to 600 °C, or ii) because of the small amount of liquid in them and/or their small size it proved impossible to measure the ice melting temperature and hence to calculate the salinity

small amount of pure CO_2 has been observed ($TmCO_2$ −56.6 °C). However, the absence of liquid CO_2 at room temperature implies a CO_2 content of much less than 2 mol % for the saline fluids (*Bowers* and *Helgeson*, 1983; *Shepherd* et al., 1985). The salinity of these fluids varied from < 23 up to 64 wt % NaCl eq. Salinity is based on Tm_{halite}. Too small an amount of the liquid phase prevented determination of Tm_{ice} (and salinity) for inclusions with no halite DM. Most of the saline Fls (V+L+DM) did not show vapour/liquid homogenisation even when heated up to 600 °C (the limit of the stage used). Only a few V+L inclusions (without DMs) homogenised to vapour at about 400 °C. Halite dissolution occurred from 186 to 532 °C. A few measured Te values (−52 to −72 °C) suggest substantial amounts of $CaCl_2$ in the captured fluid (*Shepherd* et al., 1985).

Type III. (L+V±CM) inclusions are aqueous liquid-rich Fls (degree of fill F = 0.8–0.095), with occasional small crystals of mostly unidentified insoluble (captive?) minerals. Microthermometric measurements showed a wide range of salinity (1–25 wt % NaCl eq.) but a narrow range of Th (188–283 °C – always to liquid). Te varied much in the interval −28 to −84 °C). Lower values of Te again suggest a substantial amount of $CaCl_2$ (*Shepherd* et al., 1985) in more saline fluids.

It was usually difficult to assign a primary or secondary origin to these inclusions, as most of them occur randomly within quartz grains, a typical feature of Fl in igneous quartz (e.g. *John*, 1989; *Frezzotti*, 1992; *Ratajesky* and *Campbell*, 1994). Although this observation might suggest a primary origin, a secondary origin is more likely, based on the absence of devitrified melt and subsolidus Th (< 570 °C) in most of these aqueous inclusions, as would be expected for primary Fls in magmatic quartz. The rare occurrence of crosscutting planes of Fls might be

explained by recrystallisation of the host quartz, although no petrological evidence was seen for this in the studied samples, or by migration of aqueous Fls after trapping in a thermal, pressure or gravitational gradient (for details see *Roedder*, 1984). However, most of the type III inclusions (liquid-rich and lower salinity) and some of the type II inclusions (vapour-rich without DMs only) are believed to be later than most of the type I inclusions (high salinity liquid-rich). This is supported by the fact, that type III and some of the type II inclusions have much lower Th values and are usually highly irregular in shape as they did not have enough time to re-equilibrate to more regular morphologies (*Shepherd* et al., 1985). In this context it is also necessary to stress the apparent genetic link between the saline liquid-rich (type I) and saline vapour-rich (some of type II) inclusions, that suggest aqueous immiscibility phenomena.

Skarn minerals

For the Fl study of *skarn minerals* 144 individual Fls, mostly two phase liquid-vapour type (L+V) were selected and measured. In contrast to Fl data from the granodiorite no Fl with true daughter minerals were found in any skarn mineral. The average size of Fls varied from 10 to 30 µm in their longest dimension, although some extremely large (up to 80 µm) and small (up to 5 µm) Fls have been measured. A summary of the microthermometric data is presented in Table 4 and Fig. 10.

The Fls in all types of garnet were rare to sporadic, L+V types (Fig. 7c). Relatively small differences in Th and salinity values were observed for different types of garnet. A few extremely low Th values from Fls in garnet probably reflect leakage or a secondary origin. Salinity of primary Fls in garnets varied from 4 to 23 wt% NaCl eq. and Th varied from 218 to 371 °C. The composition of fluids trapped in garnets is probably a mixture of NaCl, $FeCl_2$, $CaCl_2$, KCl and $MgCl_2$ (based on Te values between −37 and −59 °C).

The Th of rare primary L+V Fls in late epidote from epidote-calcite veins varied form 353 to 364 °C with salinity > 26 wt% NaCl eq. (Tm_{ice} observed from

Table 4. *Summary of microthermometric data from fluid inclusions in the skarn minerals.* sec. Fl *secondary fluid inclusions*, Tm – ice *temperature of first ice melting*, Th *homogenisation temperature*, Te *eutectic temperature*, n *number of inclusions measured*

	Tm - ice (°C)			Salinity (wt. % NaCl eq.)		Th (°C)			Te (°C)		
Mineral	n	range	mean	range	mean	n	range	mean	n	range	mean
Garnet I.	9	-6.9 ↔ -9.7	-8.9	10.4 ↔ -13.6	12.8	9	291 ↔ 371	335	1	-36.5	-36.5
Garnet II.	15	-3.4 ↔ -18.1	-11.6	5.5 ↔ -21.0	15.1	13	218 ↔ 326	288	7	-41 ↔ -59	-49.5
Garnet III.	6	-2.3 ↔ -20.6	-8.5	3.8 ↔ -22.8	11.2	5	219 ↔ 331	306	1	-37	-37
Garnet II. or III.	4	-3.6 ↔ -11.2	-6.5	5.8 ↔ -15.2	9.5	3	245 ↔ 355	306	-	-	-
Garnet sec. FI	4	-0.2 ↔ -6.9	-2.1	0.3 ↔ 10.4	3.2	3	233 ↔ 256	245	-	-	-
Epidote	5	-25.6 ↔ -30.4	-27.4	25.8 ↔ >26.6	26.8	5	353 ↔ 364	357	2	-63 ↔ -71	-67
Sphalerite	2	-2.4 ↔ -2.5	-2.5	3.9 ↔ 4.1	4	2	290 ↔ 295	293	-	-	-
Sphalerite sec. FI	4	-0.2 ↔ -0.6	-0.4	0.3 ↔ 1.0	0.7	4	267 ↔ 273	270	-	-	-
Quartz	46	0 ↔ -2.5	-0.9	0 ↔ 4.1	1.5	45	222 ↔ 383	285	3	-22 ↔ -33	-26
Calcite	48	0 ↔ -1.5	-0.7	0 ↔ 2.5	1.1	46	216 ↔ 371	268	4	-24 ↔ -32	-28

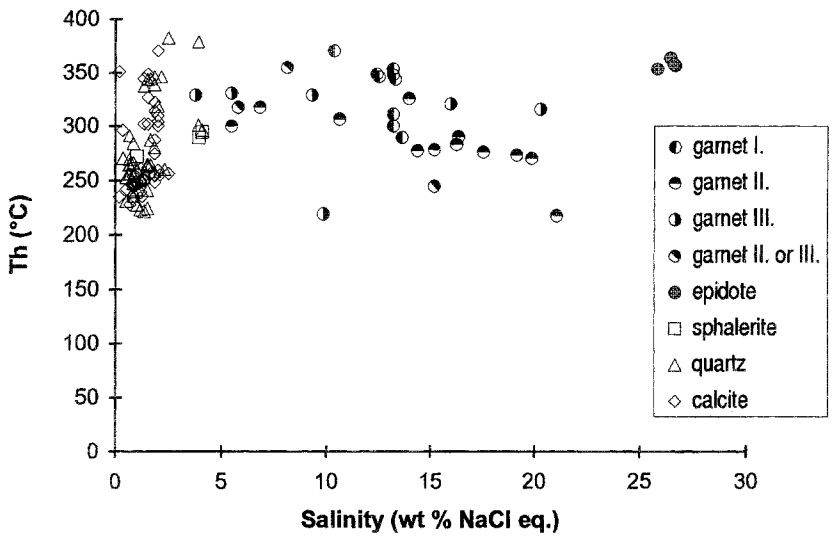

Fig. 10. Homogenisation temperature (Th) vs. salinity diagram for fluid inclusions (Fl) in skarn minerals, including various generations of garnet. All classes of Fls are included

−26 to −30 °C), although no DMs were present. Very low Te (−63, −71 °C) and Tm_{ice} (~ −27.4 °C) suggest a substantial amount of $CaCl_2$ (*Shepherd* et al., 1985), or $LiCl_2$ (*Crawford*, 1981).

Retrograde hydrothermal processes have been examined from abundant Fls in different samples of quartz, calcite and sphalerite. All the measured Fls in quartz and calcite showed very dilute, but still relatively high temperature fluids. Variable liquid-to-vapour ratios in both primary and secondary L+V Fls were observed here (Fig. 7d). The salinity of these fluids is commonly < 2 wt% NaCl eq. (max. 4 wt% NaCl eq.). The Th varied from 216 up to 383 °C. In the sample of quartz-calcite-hematite assemblage some of the vapour-rich Fls in quartz homogenised to vapour at similar Th values to those of the coexisting liquid-rich Fls (approx. 297 °C); some either homogenised to vapour at higher temperatures (300–350 °C) or displayed critical behaviour at ~ 380 °C. Their presence is taken as evidence for boiling or "unmixing" (*Ramboz* et al., 1982; *Shepherd* et al., 1985). The most frequently observed indications of boiling were found in the quartz-calcite-garnet assemblage, but here the lowest Th values for primary Fls in quartz were only ~ 222 °C. No evidence of boiling was found in the youngest hydrothermal veinlets. The Te of these fluids ranged from −33 to −22 °C (NaCl±KCl, $MgCl_2$ probably present; *Shepherd* et al., 1985). In the largest vapour-rich Fls a small amount of pure CO_2 has been observed (with $TmCO_2$ −56.6 °C, $ThCO_2$ to vapour +4.1 °C). Interestingly, in many Fls in quartz, fibrous captive minerals were also present; these did not dissolve during heating. Based on SEM-EDS studies these captive minerals were identified as sericite and halloysite? as Si, Al, K and Si, Al are present in these minerals (Fig. 7f).

In sphalerite, limited Fl data are available but two populations of L+V Fls are inferred, one with a salinity of 4 wt% NaCl eq. and Th at 293 °C (to liquid) and the

second (considered secondary) with a salinity of 0.7 wt % NaCl eq. and Th at 270 °C (to liquid).

Discussion

Evolution of magmatic aqueous fluids in granodiorite

In magmatic-hydrothermal systems, experiments have shown that an aqueous fluid exsolves from a silicate melt in response to pressure decrease or crystallisation (*Burnham*, 1979). At relatively low pressures (< 1.3 kb) the fluid might exsolve from a crystallising melt into separate vapour and liquid phases, since the P-T projection of the granodiorite minimum melting curve overlaps the P-T condition for immiscibility in the NaCl-H_2O system (*Pitzer* and *Pabalan*, 1986; *Shinohara*, 1994). Evidence for fluid immiscibility, based on Fl studies, have been described in many examples of skarn, porphyry and granite-related deposits (e.g. *Kwak*, 1986; *Layne* and *Spooner*, 1991; *Jamtveit* and *Andersen*, 1993).

The present Fl data from quartz in the granodiorite demonstrate the co-existence of very saline liquid-rich and vapour-rich Fls, as well as a large variation in Th between these two end-member types, providing strong evidence for aqueous fluid immiscibility during the early, hydrothermal stages of fluid evolution. It is noteworthy that the total homogenisation temperatures of the saline liquid-rich Fls (type I) do not exceed 572 °C (usually 460–550 °C) and are far below the accepted granodiorite solidus temperature (*Burnham*, 1979). On the other hand, most of the liquid-rich inclusions (type II) did not homogenise below 600 °C. However, we believe that these usually represent mixed portions of immiscible fluids (liquid and vapour) and therefore their Th values are anomalously high. The presence of gaseous CO_2 in these type II Fls may further increase the immiscibility region to higher temperatures (*Bowers* and *Helgeson*, 1983). In summary, it is probable, that most of the Fls in granodiorite quartz do not represent the very early exsolved magmatic fluid from the crystallising granodiorite melt. More probably they represent later evolved aqueous fluids, which subsequently unmixed. As yet there are no direct data for the PVTX properties of early magmatic (primary) fluids.

If most of the captured saline fluid is secondary, as suggested above, some interaction with the host rock has probably taken place and in consequence the chemistry has been modified to some extent. The presence of DMs and the low Te Values (−52 to −72 °C) shows that this fluid belongs to the multicomponent system H_2O-NaCl-KCl-$FeCl_2$±$CaCl_2$. The major difference from typical magmatic brine (NaCl-KCl±$FeCl_2$; *Burnham*, 1979) is the unusually high iron content, as demonstrated by the presence of several Fe-bearing daughter minerals. Although no quantitative fluid chemistry data are reported here, there are parallels with the Granisle porphyry copper deposit, where chemical analyses of Fls with a similar variety of DMs showed $FeCl_2$ contents between 31 to 45 wt%, and total salinity up to 84 wt% of NaCl+KCl+$FeCl_2$ (*Quan* et al., 1987). Similar values for $FeCl_2$ content and total salinities might be expected for the Fls in granodiorite quartz from the Vyhne-Klokoč deposit. Although salinities calculated here using halite dissolution temperatures alone, are somewhat lower (max. 68 wt% NaCl eq.).

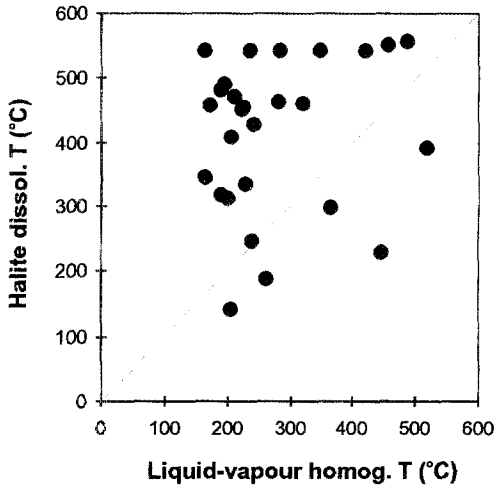

Fig. 11. Halite dissolution temperatures as a function of liquid-vapour homogenization temperatures for halite bearing type I. and II. inclusions. Most inclusions undergo L-V homogenization far below halite dissolution temperatures probably as a result of the substantial presence of iron chlorides in the captured fluids

Very high iron contents in inclusion fluids places limitations on the interpretation of their P-T properties. Experimental data is not available for the system NaCl-KCl-$FeCl_2$-H_2O, and the simpler NaCl-H_2O system (*Bodnar*, 1994) is not really appropriate for modelling more complex chemical systems, as already stated by *Campbell* et al. (1995). *Bodnar* (1994) determined the slope of the liquid plus halite isochore for inclusions with 40 wt% NaCl which homogenise by halite disappearance to be between 20 and 25 bars/°C. If Bodnar's data are extrapolated to the higher salinities in the present study, the inclusions in which Tm_{halite} is 300 °C greater than Th_{vapour} (Fig. 11) would have to have formed at about 6 to 7.5 kbar. This pressure is unrealistically high considering the geologic constraints.

High iron content in saline Fls could be explained by subsolidus fluid-rock equilibrium reactions. According to the experimental work of *Whitney* et al. (1985), at between 650 and 500 °C iron accounts for up to 50% of the available chlorine in fluids in equilibrium with rocks of granitic composition. This determination is also supported by the high solubility of Fe chlorides in high temperature saline fluids (*Eugster*, 1985; *Kwak* et al., 1986). So, in the Fls from the granodiorite the high iron content is in accordance with an extremely high salinity. The high Cl content is thought to result partly from aqueous fluid immiscibility, of a fluid already enriched in chlorine from an earlier (exsolved) magmatic fluid. However, the high iron content is probably, to a large extent, the result of exchange reactions with coexisting crystallised Fe-rich phases (*Whitney* et al., 1985). Petrographic and petrological evidence in the granodiorite apophyses shows that such reactions have indeed taken place (Table 1, Fig. 3). Mafic minerals (and plagioclase) have been replaced to a variable extent by chlorite, quartz, albite-rich plagioclase and dominant K-feldspar, whose low orthoclase content indicates subsolidus crystallisation (*Káčer* et al., 1995). The overall result is that iron, mobilised from fluid-mineral interactions, has further added to iron already present in an early magmatic fluid.

As the inferred fluid-rock interaction needs a sufficient water/rock ratio to be effective, it is necessary to invoke some mechanism to concentrate the magmatic

fluids in the places of equilibration. The mechanism of egress of magmatic fluids and their focusing into sites of alteration and/or mineralisation has been considered theoretically by *Candela* (1991). Two main models were presented: A. "a bubble-plume" model involving ascent of bubble-laden melt along the side of the intrusion with accompanying crystallisation and B. "an advection" model involving clusters of bubbles at critical percolation as a result of saturation in a crystallization interval within the magma chamber (for details see *Candela*, 1991). As the separation of aqueous fluid into vapour and liquid phases takes place, both phases could rise to the roof zone of the intrusion. However, because we lack data about the initial magmatic H_2O concentration we are not able to determine which of these two possible accumulation processes occurred in the granodiorite. There are clear indications for accumulation of magmatic saline liquid and vapour along the roof of the granodiorite and especially in the apophyses, that worked as natural trap for rising magmatic fluids. High magmatic water/rock ratio in apophyses enabled extensive equilibrium reactions between the fluid and rock as described above.

An overlap exists between the microthermometry data from late secondary Fls (type III) in the granodiorite quartz and primary Fls in garnets (Fig. 12), indicating similar fluid sources. In the absence of stable isotope data the source of metasomatic fluids can only be inferred from the Th/salinity evolution paths of Fls in granodiorite quartz. The fact that higher salinity and Th inclusions (type I) seem to be earlier than lower salinity and Th inclusions (type III), suggests that substantial mixing with dilute and cooler fluids, probably of meteoric origin, occurred after equilibration of early magmatic fluids. The continuity of this process is suggested by the simultaneous decrease of both salinity and Th values (Fig. 9).

The substantial mixing of magmatic and meteoric fluids together with early hydrothermal immiscibility and possible late hydrothermal boiling phenomena

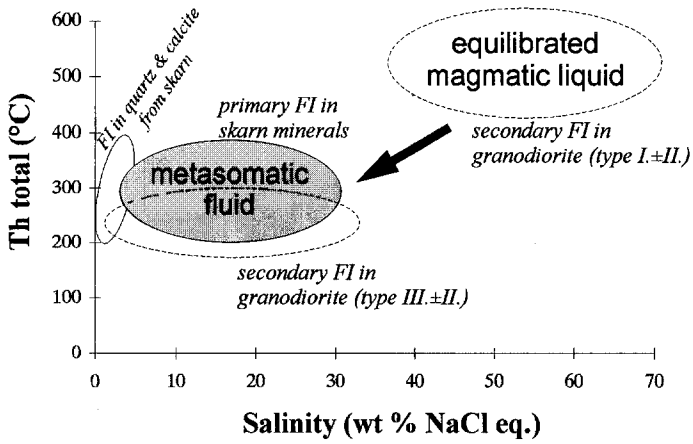

Fig. 12. Total homogenisation temperature (Th_{total}) vs. salinity diagram for all the main groups of fluid inclusions (Fl). Overlapping groups of primary Fls in skarn minerals and type III. Fls in granodiorite quartz are derived from the dense saline magmatic liquid that equilibrated with granodiorite apophyses and was captured in type I. inclusions. Fls in quartz and calcite from skarn (both primary and secondary) represent late hydrothermal fluids with dominant features of boiling and dilution

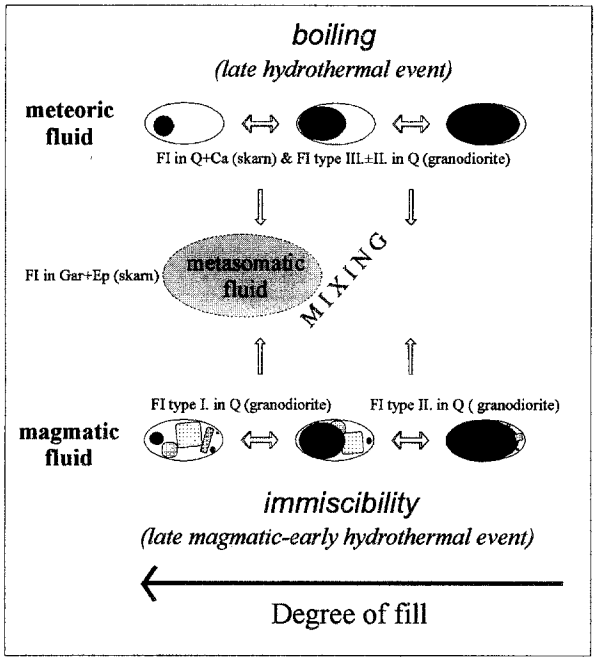

Fig. 13. Schematic fluid evolution model showing the relationship between different types of fluid inclusions (FI) and fluids reflecting the immiscibility, boiling and mixing phenomenons. Skarn-forming metasomatic fluid probably originated from substantial mixing of magmatic and meteoric waters (see text for details). *Q* quartz, *Ca* calcite, *Gar* garnet, *Ep* epidote

explains the presence of all the types of inclusions captured in granodiorite quartz (Fig. 13).

Characterisation of fluid in the skarn environment

The fluid inclusion study of garnet and epidote provide information on the character of fluids responsible for the skarn mineralisation. Fluid inclusions with high salinity and Th values are absent. No evidence of fluid immiscibility, i.e. boiling, has been observed in the skarn mineral assemblages except in the very late hydrothermal quartz and calcite.

Grossularite-andradite garnets and their complex zoning are sensitive to even small changes in fluid composition and should therefore mirror the fluid evolution in skarn assemblages (*Jamtveit* et al., 1993). Primary FIs from each type of garnet show large variations in the salinity (4–23 wt% NaCl eq.) and Th (219–371 °C) that appears to be mostly independent of the mineralogically and texturally distinct garnet types (Fig. 5). Only the early garnet (garnet I) differs somewhat from the other types of garnet in having a slightly increased Th range. The observed broad variation in salinity and Th in these fluids could be related to different levels or depths of formation of the garnets in relation to the contact, but this was not possible to prove since most samples were taken from mine dump material. Alternatively, the variations can result from the interaction of an original saline magmatic fluid with some more dilute but hot fluids, possibly heated meteoric waters.

Primary FIs from the late epidote showed slightly higher Th and salinity values than those in earlier garnets. As the late epidote occurs in veinlets the increased salinity could be explained by the penetration of more saline fluids from depth, using relatively deeper faults, connected with the cooling of the intrusion during the retrograde stage.

Significant $CaCl_2$ contents ($Te < -50\,°C$) and low CO_2 contents were identified in many skarn-hosted Fls and granodiorite-hosted Fls. These are typical components for any skarn-forming fluids (*Einaudi* et al., 1981; *Kwak*, 1986). High $CaCl_2$ contents are possibly caused by the equilibrium reaction of magmatic fluids with granodiorite below 400 °C (*Whitney* et al., 1985). This is probably related to the decomposition of plagioclase in the granodiorite apophyses. The source of minor gaseous CO_2 is believed to be magmatic because this phase was also detected in some gas-rich Fls in granodiorite quartz (type II.). However, it is also possible that the high $CaCl_2$ contents and the presence of minor gaseous CO_2 is caused by rapid decarbonation reactions in marbles during the metasomatic processes of skarn evolution (*Kwak*, 1986).

Boiling in late retrograde quartz and calcite probably reflects substantial progressive erosion of the overlying volcano before caldera collapse (*Lexa* et al., in press). The thickness of the precaldera volcanic complex in the central zone of the stratovolcano varies between 300–1000 m (*Konečný* et al., 1993), while paleovolcanic reconstruction indicates an original volcano height of >2000–3000 m (*Konečný* et al., 1995). Decreasing depth at relatively constant temperature had the effect of approaching the necessary pressure limit for boiling in a hydrothermal column (*Haas*, 1971). Boiling might account for the non-equilibrium crystallisation of skarn minerals in the retrograde stage. Simultaneous boiling and dilution occurred from 300 to 220 °C finally resulting in simple dilution, as is apparent from the Th vs. salinity plot (Fig. 10).

The evidence for boiling in retrograde quartz and calcite permits us to regard the Th values as the true trapping temperatures of the fluid (*Shepherd* et al., 1985) and to calculate the pressure and depth at the time of precipitation of the final stage of mineralisation. For the pressure estimate, minimum Th and average salinity of primary Fls in quartz were used. Applying the equations of *Brown* and *Lamb* (1989) the pressure calculation for boiling fluid yields 78 bars (for 4 wt% NaCl eq., 297 °C – quartz-calcite-hematite asemblage) and 24 bars (for 1.3 wt% NaCl eq., 222 °C – quartz-calcite-garnet assemblage). These correspond to depths of 800 and 250 m respectively assuming hydrostatic conditions (*Haas*, 1971) or depths of 300 and 90 m assuming lithostatic conditions. The calculated pressures in both cases represent "minimum" values, because of the presence of CO_2 gas in some of the "boiling" Fls. The addition of even small amounts of CO_2 to H_2O-NaCl fluids significantly raises the vapour pressure and concomitantly the depth of formation (*Bodnar* et al., 1985). As there is no supporting evidence of filled fractures in the overlying Choč nappe sediments, it cannot be assumed that the fractures were open up to the surface and under purely hydrostatic pressure. Therefore a pressure/depth estimate somewhere between hydrostatic and lithostatic is most probable.

Even if there is a large inaccuracy in the depth estimate, the Vyhne-Klokoč skarn can be clearly classified as a shallow skarn type deposit (*Kwak*, 1986). The shallow depth is also implied by the lack of high PT metamorphism in surrounding rocks, widespread skarn-formation and brittle features including hydrothermal veining and brecciation (*Hickey*, 1992). Relatively low pressures, and consequently the shallow setting for skarn formation is also supported by the presence of extremely saline Fls in granodiorite quartz, since in the system silicate melt-

exsolving immiscible fluid the major amounts of Cl are distributed to the liquid phase particularly at lower pressures (*Shinohara*, 1994).

Low pressure conditions indicate only a small pressure correction to Th of Fls from skarn minerals to estimate the true trapping temperature (*Shepherd* et al., 1985). This assertion is confirmed also by the independent chlorite geothermometer (Fig. 6). The calculated temperatures of chlorite crystallisation are in good agreement with Th values from skarn mineral Fls.

Relationships between fluids of magmatic origin and skarn-forming fluids – an integrated model

In the following two stage model (Fig. 14) the Fl data both from the skarn and the granodiorite are integrated with the geological, petrological and mineralogical observations. In this model, the assumption is made that the iron within the skarns is derived from a dense saline liquid, exsolved and evolved from the granodiorite melt and equilibrated with preexisting mineral phases (Fig. 12). The possibility that iron is transported in the coexisting vapour phase is discounted because of the low capacity of Cl-poor vapour to carry Fe-chloride complexes (*Hemley* et al., 1992; *Shinohara*, 1994).

In order to model fluid evolution at the Vyhne-Klokoč skarn deposit it is necessary to emphasise its position inside the stratovolcano structure and the consequent hydrodynamic regime during the time of granodiorite intrusion emplacement and related skarn formation (Fig. 14, based *Lexa* et al., in press). At the time of emplacement meteoric waters probably circulated through the upper volcanogenic sequences along the slopes of the volcano, but did not approach the hot granodiorite, because of its thermal aureole. Later, cooling of the intrusion allowed meteoric waters to approach its margins, but the direction of the circulation in the sedimentary basement sequences is not entirely clear (see Fig. 14 – lower left corner). Either the hydraulic pressure pushed the meteoric waters down to the granodiorite reflecting the stratovolcanic morphology (arrow labelled A) or the margins of the intrusion were approached from the opposite direction by deep circulating heated meteoric waters (arrow labelled B). Both possibilities are in accordance with models of volcanogenic ore deposits in stratovolcanic setting (e.g. *Hedenquist* and *Lowenstern*, 1994).

In the first part of the model during supersolidus conditions (Fig. 14 part 1) immiscible aqueous fluid exsolved from the crystallising granodiorite and concentrated at the roof of the intrusion, especially in apophyses, by mechanisms described by *Candela* (1991). The very saline liquid, resulting from immiscibility, is buoyant within the magmatic system ($\rho_{melt} > \rho_{fluid}$), but is not buoyant within a typical hydrothermal system (*Henley* and *McNabb*, 1978; *Candela*, 1991). The high density of this liquid ($\rho \geq 1.2$, modelled on a simple NaCl-H_2O system) probably restricted significant flow of saline liquid into the surrounding basement rocks so that remained predominantly captured in the cooling granodiorite apophyses. In this early stage the basement rocks were probably affected by minor recrystallisation and skarnisation int he proximity of the apophyses, as only the vapour phase (or its condensates) could contribute to the early contact metasomatic processes in limestones. However, the contribution of magmatic

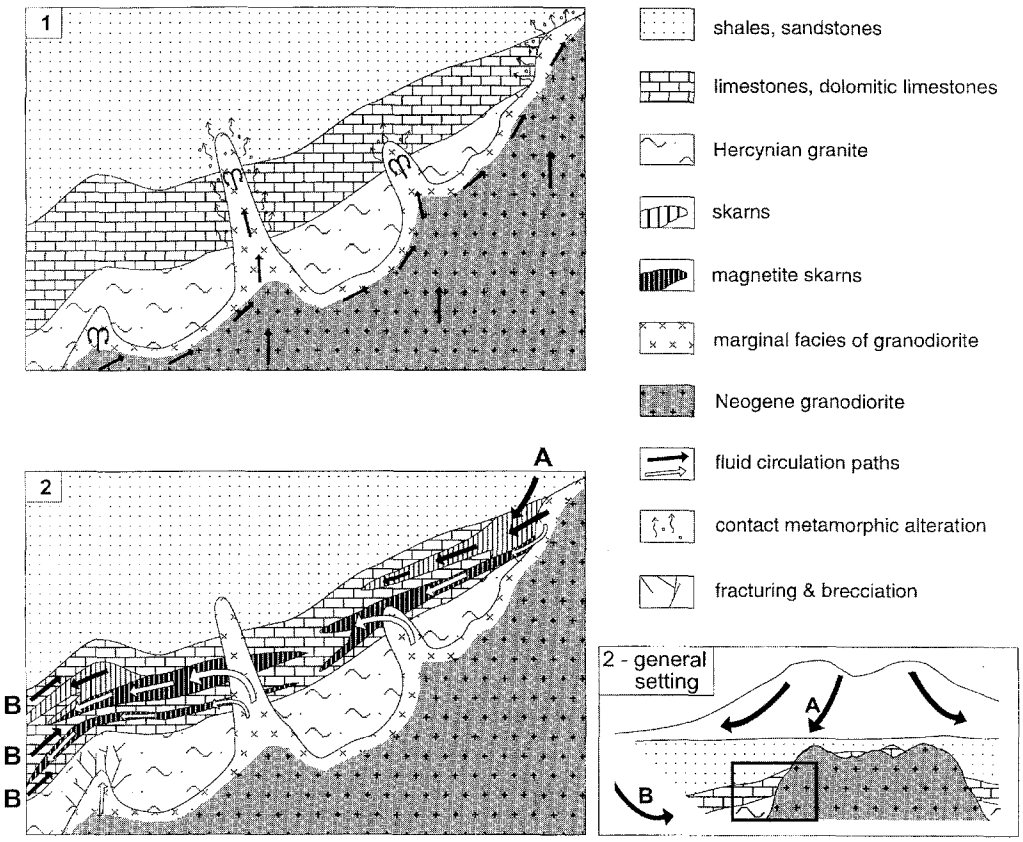

Fig. 14. Schematic model for fluid and skarn evolution at the Fe-skarn Vyhne-Klokoč deposit. The general setting inside the Štiavnica stratovolcano during the skarn-forming process is shown in the lower right corner including its expected hydrodynamic regime of meteoric fluids (marked by arrows). It is not clear, which of the marked circulation paths (labelled A and B) occurred during the skarn formation and diluted the ponded magmatic fluids inside the apophyses. 1. supersolidus stage, 2. subsolidus stage

vapour to the early skarn formation is hypothetical, as no relevant Fls were found in any skarn mineral.

Later decreasing temperature during subsolidus conditions (Fig. 14, part 2) produced disequilibrium of accumulated fluid in the apophyses with pre-existing mineral phases. Consequently, fluid-mineral equilibrium reactions occurred resulting in leaching of iron from the mafic mineral phases and its addition to the accumulated saline fluid. Further cooling of the intrusion and transition to hydrothermal pressure conditions allowed circulating meteoric waters to approach the margins of the granodiorite and to penetrate substantially into the apophyses inside sedimentary basement rocks. This had the effect of decreasing the salinity and density of the ponded, equilibrated magmatic fluid (Fe-bearing brine), thus

making it more buoyant and able to move outward into the basement sequences. Once diluted magmatic fluids entered the limestones, metasomatic skarn reactions started along the fluid paths on the contact with limestones. Although the direction of the diluting meteoric fluids cannot be determined (Fig. 14A or B), the direction of the skarn-forming fluid must have been downwards, because of the greater density of the more saline metasomatic fluid compared to the meteoric one. More or less acid Fe-bearing metasomatic fluids precipitated magnetite and other Fe-rich exoskarn minerals in response to neutralisation (*Kwak* et al., 1986). The fluid inclusion study supports the above assertion. There is an absence of very saline Fls in any skarn mineral, but there is an overlap between the Fl data from primary Fls in garnets and late secondary Fls in the granodiorite quartz (type III.), indicating the same source for the hydrothermal fluids, probably a mixture of magmatic and meteoric waters (Fig. 12). The shape of the skarn lenses, parallel to the slope of the basement sequences (Fig. 2b) might indicate lateral flow of the skarn-forming fluids. Although the shape could be a function of the composition of the hosting Vel'ký Bok sedimentary group, as some minor non-carbonate sequences are present along with the dominant carbonates.

Granodiorite apophyses that terminated inside impermeable basement rocks of the Hercynian granite, probably followed a different scenario compared to that terminated inside sedimentary basement sequences. Here, owing to crystallisation the pressure of the evolving magmatic fluid considerably exceeded the lithostatic pressure and the saline iron-bearing fluid was expelled from the carapace of the granodiorite apophyses (models of *Burnham*, 1979 and *Jamtveit* and *Andersen*, 1993). Local hydraulic fracturing and brecciation in the Hercynian granite, accompanied by tourmaline and quartz filling, could be attributed to this process.

Increased influx of meteoric waters inside the granodiorite apophyses had the effect of further diluting of original, saline, magmatic fluid. Outside the apophyses this resulted in precipitation of late retrograde skarn and hydrothermal mineralizations, replacing older skarn mineral assemblages. Contemporaneous progressive erosion of the overlying volcano had the effect of reducing the pressure to that necessary for boiling, and this was associated with the precipitation of late stage retrograde mineralization. In the granodiorite, late meteoric fluids were probably responsible for late hdydrothermal alteration including growth of sericite and clay minerals.

Acknowledgements

This research has been carried out as a part of the project "Mineral resources of Slovakia", number ZP-547–010 funded by the Slovak Science and Technology Fund, and simultaneously as a part of a postgraduate research at the School of Geological Sciences, Kingston University. We are grateful to the British Council, Bratislava and RTZ Mining and Exploration Ltd. for funding co-operation between the School of Geological Sciences, Kingston University and the Geological Survey of the Slovak Republic, Bratislava (former Dionýz Štúr Institute of Geology). Dr. *S. Roberts* (Southampton University) helped with Laser Raman analysis. The mineralogical part of this study was realized under supervision of *M. Chovan* (Department of Mineralogy and Petrology at the Comenius University, Bratislava). The manuscript was improved by the comments of *P. J. Treloar*, *D. H. M. Alderton* and *M. Feely*.

References

Afifi AM, Essene EJ (1988) MINFILE: a microcomputer program for storage and manipulation of chemical data on minerals. Am Mineral 73: 446–448

Bayliss P (1975) Nomenclature of the trioctahedral chlorites. Can Mineral 13: 178–180

Bodnar RJ (1994) Synthetic fluid inclusions XII. The system H_2O-NaCl. Experimental determination of the halite liquidus and isochores for a 40 wt percent NaCl equiv solution. Geochim Cosmochim Acta 5: 1053–1064

Bodnar RJ, Reynolds TJ, Kuehn CA (1985) Fluid inclusion systematics in epithermal systems. In: *Berger BR, Bethke PM* (eds) Geology and geochemistry of epithermal systems. Rev Econ Geol 2: 73–97

Bowers TS, Helgeson HV (1983) Calculation of the thermodynamic and geochemical consequences of nonideal maxing in the system H_2O-CO_2-NaCl on phase relations in geological systems: equation of state for H_2O-CO_2-NaCl fluids at high pressures and temperatures. Geochim Cosmochim Acta 47: 1247–1275

Brown PE (1989) FLINCOR: a microcomputer program for the reduction and investigation of fluid-inclusion data. Am Mineral 74: 1390–1393

Brown PE, Lamb WM (1989) P-V-T properties of fluids in the system H_2O-CO_2-NaCl: new graphical presentations and implications for fluid inclusion studies. Geochim Cosmochim Acta 53: 1209–1221

Burnham CW (1979) Magmas and hydrothermal fluids. In: *Barnes HL* (ed) Geochemistry of hydrothermal ore deposits, 2nd ed. Wiley, New York, pp 71–136

Campbell AR, Banks DA, Phillips RS, Yardley BWD (1995) Geochemistry of the Th-U-REE mineralizing fluid, Capitan Mountains, New Mexico, U.S.A. Econ Geol 90: 1273–1289

Candela PA (1991) Physics of aqueous phase evolution in plutonic environments. Am Mineral 76: 1081–1091

Cathelineau M (1988) Cation site occupancy in chlorites and illites as a function of temperature. Clays Minerals 23: 471–485

Cathelineau M, Nieva D (1985) A chlorite solid solution geothermometer. The Los Azufres geothermal system (Mexico) geothermal field. Contrib Mineral Petrol 91: 235–244

Chou, I-M (1987) Phase relations in the system NaCl-KCl-H_2O. III. Solubilites of halite in vapor saturated liquids above 445 °C and redetermination of phase equilibrium properties in the system NaCl-H_2O to 1000 °C and 1500 bars. Geochim Cosmochim Acta 51: 1965–1975

Crawford ML (1981) Phase equilibria in aqueous fluid inclusions. In: *Hollister LS, Crawford ML* (eds) Fluid inclusions: applications to petrology. Mineralogical Association of Canada Short Course Handbook 6: 75–100

Dong G, Pollard PJ (1997) Identification of ferropyrosmalite by Laser Raman microprobe in fluid inclusions from metalliferous deposits in the Cloncurry District, NW Queensland, Australia. Mineral Mag 61: 291–293

Einaudi MT, Burt DM (1982) Introduction – terminology, classification, and composition of skarn deposits, Econ Geol 77: 745–754

Einaudi MT, Meinert LD, Newberry RJ (1981) Skarn deposits. Econ Geol (75th Anniv Vol): 317–391

Eugster HP (1985) Granites and hydrothermal ore deposits: a geochemical framework. Mineral Mag 49: 7–24

Frezzotti ML (1992) Magmatic immiscibility and fluid phase evolution in the Mount Genis granite (southeastern Sardinia, Italy). Geochim Cosmochim Acta 56: 21–33

Gavora S (1962). Magnetitové ložisko vo Vyhniach. Geol Práce Zošity 62: 305–308

Gavora S, Hrušković S (1963) Skarnové ložiská vo vulkanitoch Štiavnického pohoria v oblasti Hodruša-Vyhne. Geol Práce Zprávy 29: 133–142

Gavora S, Lukaj M (1968) Vyhne – Fe. Záverečná správa o vyhľadávacom prieskume a vypočet zásob so stovom k 31. 12. 1968. Internal final report, Geofond, Bratislava

Hass JL (1971) The effect of salinity on the maximum thermal gradient of a hydrothermal system at hydrostatic pressure. Econ Geol 66: 940–946

Hall DL, Sterner SM, Bodnar RJ (1988) Freezing point depression of NaCl-KCl-H_2O solutions. Econ Geol 83: 197–202

Hedenquist JW, Lowenstern JB (1994) The role of magmas in the formation of hydrothermal ore deposits. Nature 370: 519–527

Hemley JJ, Cygan GL, Fein JB, Robinson RB, D'Angelo WM (1992) Hydrothermal ore-forming processes in the light of studies in rock-buffered systems I. Iron-copper-zinc-lead sulfides solubility relations. Econ Geol 87: 1–22

Henley RW, McNabb A (1978) Magmatic vapor plumes and ground-water interaction in porphyry copper emplacement. Econ Geol 73: 1–20

Hickey III RJ (1992) The Buckhorn Mountain (Crown Jewel) gold skarn deposit, Okanogan County, Washington. Econ Geol 87: 125–141

Jamtveit B, Andersen T (1993) Contact metamorphism of layered shale-carbonate sequences in the Oslo Rift. III. The nature of skarn-forming fluids. Econ Geol 88: 1830–1849

Jamtveit B, Wogelius RA, Fraser DG (1993) Zonation patterns of skarn garnets: records of hydrothermal system evolution. Geology 21: 113–116

John DA (1989) Geologic setting, depths of emplacement, and regional distribution of fluid inclusions in intrusions of the central Wasatch Mountains, Utah. Econ Geol 84: 386–409

Káčer Š, Koděra P, Hojstričová V, Lexa J (1993) Zhodnotenie Fe-skarnových mineralizácií v centrálnej zóne štiavnického stratovulkánu. Internal report of D. Štúr Institute of Geology, Bratislava, 67 p

Káčer S, Koděra P, Konečný P, Lexa J (1995) Fe-skarnová mineralizácia. In: *Onačila D* et al. (eds) Metalogenetický model a prognózne zhodnotenie centrálnej zóny štiavnického stratovulkánu. Internal report of D. Štúr Institute of Geology, Bratislava pp 83–97

Koděra P (1994) Fe – bearing skarns. In: *Chovan M, Háber M, Jeleòň S, Rojkovič I* (eds) Ore textures in the Western Carpathians. Slovak Academic Press, Bratislava, pp 83–90

Koděra P, Chovan M (1994) Mineralogicko-paragenetické pomery skarnového ložiska Vyhne-Klokoč. Mineralia Slovaca 26: 38–49

Konečný V, Planderová E, Lexa J (1983) Stratigraphy of the Central Slovakia Neogene Volcanic Field. Západ Karpaty Sér Geol 9: 1–205

Konečný V, Lexa J, Hók J, Vozárová A, Vozár J, Onačila D, Štohl J, Hojstričová V, Podoláková S (1993) Geologická mapa centrálnej zóny štiavnického stratovulkánu v mierke 1:10 000. Vysvetlivky. Internal report of D. Štúr Institute of Geology, Bratislava

Konečný V, Lexa J, Hojstričová V (1995) The Central Slovakia Neogene volcanic field: a review. Acta Vulcanol 7(2): 63–78

Kwak TAP (1986) Fluid inclusions in skarns (carbonate replacement deposits). J Metamorph Geol 4: 363–384

Kwak TAP, Brown WM, Abeysinghe PB, Tan TH (1986) Fe solubilities in very saline hydrothermal fluids: their relations to zoning in some ore deposits. Econ Geol 81: 447–465

Layne GD, Spooner ETC (1991) The JC tin skarn deposit, southern Yukon Territory. I. Geology, paragenesis, and fluid inclusion microthermometry. Econ Geol 86: 29–47

Lexa J, Konečný V, Kaličiak M, Hojstričová V (1993) Distribúcia vulkanitov karpatskopanónskeho regiónu v priestore a čase. In: *Rakús M, Vozar J* (eds) Geodynamický model a hlbinná stavba Západných Karpát. D. Štúr Institute of Geology, Bratislava, pp 57–69

Lexa J, Konečný P, Hojstričová V, Konečný V, Macinská M (1997) Petrologický model štiavnického stratovulkánu. Internal report of Geol Survey of Slovak Republic, Bratislava

Lexa J, Štohl J, Konečný V (in press) Banská Štiavnica ore district: relationship among metallogenetic processes and geological evolution of the central volcanic zone. Mineral Deposita 34

Onačila D, Marsina K, Rojkovičová L', Káčer Š, Hojstričová V, Žáková E, Štohl J, Konečný V, Nemčok M, Koděra P, Konečný P, Repčok I, Hurai V, Háber M, Jeleòň S, Mat'o L', Sasváry T, Smidt R, Zvara I, Grant T (1995) Metalogenetický model a prognózne zhodnotenie centrálnej zóny štiavnického stratovulkánu. Internal report of D. Štúr Institute of Geology, Bratislava

Pirajno F (1992) Hydrothermal mineral deposits. Springer, Berlin Heidelberg New York Tokyo, 709 p

Pitzer KS, Pabalan RT (1986) Thermodynamics of NaCl in steam. Geochim Cosmochim Acta 50: 1445–1454

Quan RA, Cloke PL, Kesler SE (1987) Chemical analyses of halite trend inclusions from the Granisle porphyry copper deposit, British Columbia. Econ Geol 82: 1912–1930

Ramboz C, Pichavant M, Weisbrod A (1982) Fluid immiscibility in natural processes: use and misuse of fluid inclusion data. II. Interpretation of fluid inclusion data in terms of immiscibility. Chem Geol 37: 29–48

Ratajeski K, Campbel AR (1994) Distribution of fluid inclusions in igneous quartz of the Capitan pluton, New Mexico, USA. Geochim Cosmochim Acta 58: 1161–1174

Roedder E (1984) Fluid inclusions. Mineral Soc Am Rev Mineral 12: 644 p

Rozložník L, Jakabská K, Dauteuil D, Kosztolányi Ch, Kovách A (1991) Petrogenesis and age determination of the Hodruša granodiorite (Hodruša Hámre, Štiavnické vrchy Mts., Czecho-Slovakia). Geol Carpath 42: 77–83

Schimmel F (1928) Löslichkeiten und Umwandlungspunkte der Eisenchlorürhydrate in wäßriger Lösung. Z Anorg Chem 176: 285–288

Shepherd TJ, Rankin AH, Alderton DHM (1985) A practical guide to fluid inclusion studies. Blackie and Son, London, 235 p

Shinohara H (1994) Exsolution of immiscible vapor and liquid phases from crystallizing silicate melt: implications for chlorine and metal transport. Geochim Cosmochim Acta 58: 5215–5221

Shinohara H, Iiyama JT, Matsuo S (1989) Partition of chlorine compounds between silicate melt and hydrothermal solutions. I. Partition of NaCl-KCl. Geochim Cosmochim Acta 53: 2617–2630

Šulgan M (1986) Petrológia granodioritu hodrušsko-štiavnického intruzívneho komplexu z hl'adiska možnej rudonosnosti. Thesis, Slovak Academy of Sciences, Banská Bystrica, 120 p (unpublished)

Whitney JA, Hemley JJ, Simon FO (1985) The concentration of iron in chloride solutions equilibrated with synthetic granitic compositions: the sulfur-free system. Econ Geol 80: 444–460

Wilson JWJ, Kesler SE, Cloke PL, Kelly WC (1980) Fluid inclusion geochemistry of the Granisle and Bell porphyry copper deposits, British Columbia. Econ Geol 75: 45–61

Zábranský F (1969) Skarnové ložiská v oblasti Štiavnického ostrova. Mineralia Slov 3–4: 236–246

Authors' addresses: *P. Koděra* and *J. Lexa*, Geological Survey of the Slovak Republic, Mlynská dolina 1, 817 04 Bratislava, Slovakia; *A. H. Rankin*, School of Geological Sciences, Kingston University, Kingston-upon-Thames, Surrey KT1 2EE, United Kingdom